

Heterogeneous & Homogeneous & Bio- & Nano-

CHEM **CAT** CHEM

CATALYSIS

Accepted Article

Title: Preparation of MOF confined Ag NPs for high size selective hydrogenation of olefins

Authors: Hong Jiang, Wen-Jing Chen, Bin-Hai Cheng, and qing-Ting Sun

This manuscript has been accepted after peer review and appears as an Accepted Article online prior to editing, proofing, and formal publication of the final Version of Record (VoR). This work is currently citable by using the Digital Object Identifier (DOI) given below. The VoR will be published online in Early View as soon as possible and may be different to this Accepted Article as a result of editing. Readers should obtain the VoR from the journal website shown below when it is published to ensure accuracy of information. The authors are responsible for the content of this Accepted Article.

To be cited as: *ChemCatChem* 10.1002/cctc.201800744

Link to VoR: <http://dx.doi.org/10.1002/cctc.201800744>

Preparation of MOF confined Ag NPs for high size selective hydrogenation of olefins

Wen-Jing Chen, Bin-Hai Cheng, Qing-Ting Sun, and Hong Jiang*

Abstract: Catalysts with both high activity and good selectivity for hydrogenation of olefins to alkanes are of interest. Herein, MOF confined ultrafine Ag NPs (Ag@HKUST-1) were synthesized by double-solvent approach using HKUST-1 as the template and support. HKUST-1 with narrow cage size distribution (0.5 to 0.9 nm) confined the growth of Ag NPs, while the uniform pores prohibited the entrance of olefins with the molecular size larger than 5.0 Å, which endow the Ag@HKUST-1 with high catalytic activity and size selectivity for hydrogenation reaction. The hydrogenation of eight kinds of olefins with different molecular size (1-hexene, cyclohexene, 1-octene, cyclooctene, styrene, 1-decene, 1, 1-diphenylethylene, and 1-dodecene) catalyzed by Ag@HKUST-1 confirmed this hypothesis. The olefins with molecular smaller than 5.0 Å were efficiently converted to the corresponding alkanes, whereas those greater than 5.0 Å exhibited extremely low conversion. The catalyst also exhibited high recycle stability in the hydrogenation of styrene.

The atom economical reactions are becoming increasingly important for the chemical industry. Catalysts with both high activity and good selectivity are of interest.^[1-4] The size-selective hydrogenations are critical reactions in the petro-chemical industry whereby the molecules are absorbed in a sterically controlled fashion and selectively transformed in the uniform micropores, thus giving unusual product selectivity in various reactions.^[5-7] The size-selective reaction based on size or shape selectivity has been pursued for several decades. Various types of composite nanostructures were synthesized, typically comprising metallic nanoparticles (NPs) embedded in or covered by porous solid materials. The porous solid materials include a wide variety of structures from zeolites to amorphous carbons or porous silicon dioxide.^[8-10] However, the inorganic porous materials, such as zeolites, lack of flexibility, whereas the porous carbon materials and the porous organic polymers are mostly disordered in the pore structures, which possesses low selectivity.

Metal-organic frameworks (MOFs) with highly uniform pore shape and size are vitally valuable to size-selective catalysis: when the catalyst NPs are loaded in the pores, small and uniform reactant molecules can be accommodated and effectively converted while molecules with large size will not be able to contact with catalyst NPs. Furthermore, the small and uniform pores in MOFs may confine the growth of metal NPs during the reduction of metal ions, resulting in the uniform and ultrafine metal NPs.^[11] Meanwhile, using MOFs to confine or stabilize the metal NPs can effectively prevent the migration and agglomeration of metal NPs, thereby allowing the metal NPs to exhibit superior catalytic performance.^[12-16] Generally, NPs-MOF

composites can be prepared either by encapsulating presynthesized NPs in MOFs (building MOFs around the pre-formed NPs) or using MOFs as templates to generate NPs within their cavities.^[17-19] In the former case, usually pre-synthesized NPs are stabilized with certain surfactants, capping agents or even ions, and NPs are then encapsulated by MOF. NPs with different morphologies and sizes can be obtained by controlling the synthesis conditions of encapsulation method. However, the reported sizes of pre-synthesized NPs are usually relatively large (~20 nm). As the hydrodynamic radius of NPs is much larger than the cavity size of the MOF, most of NPs load on the surface of MOF, rather than occupy the MOF cavities, resulting low size selectivity. In the template method, the size of NPs can be less than 10 nm, but the morphology of metal NPs is relatively difficult to control and the obtained NPs are not uniform, which impairs the catalytic activity.^[20-23]

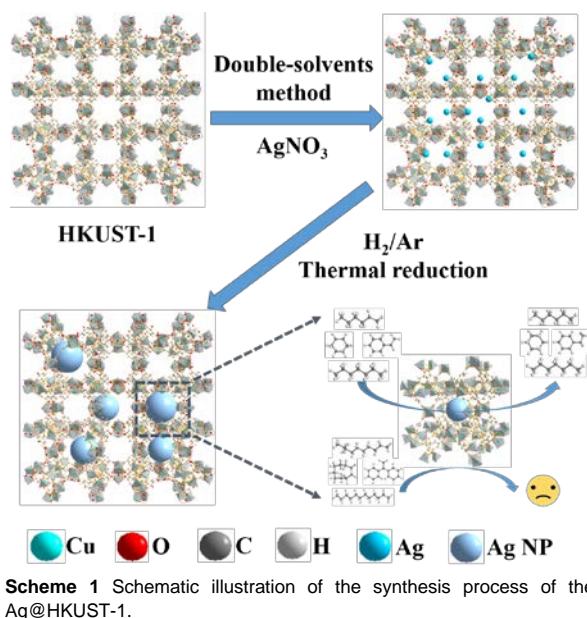
Double-solvent approach was developed to rationally introduce metal precursors into MOF pores by the capillary action and the differences in hydrophilicity inside and outside the MOF, following reduction by H₂ or other reductants to generate tiny NPs confined in MOFs. MOFs with hydrophilic internal hole were generally selected as host to be highly dispersed in a large volume of low-boiling-point and non-polar organic solvent, and then added to the metal precursor aqueous solution. Due to the hydrophilic interactions of the MOF inner pores and the capillary force, the metal precursor aqueous solution preferentially diffused into the inside hydrophilic pores of the MOFs. As long as the volume of the metal precursor is not larger than the MOF pore volume, theoretically all metal precursors can be completely incorporated into the MOF pores.^[22, 24] For instance, Xu et al. firstly and cleverly introduced metal precursors into the MIL-101 (Cr) pores by the double-solvent approach and obtained the ultrafine-sized metal NPs inside the cavities.^[25]

Herein, MOF confined Ag NPs (Ag@HKUST-1) were synthesized by double-solvent approach using HKUST-1 as the template and support (Scheme 1). The surface area, thermal stability, water stability, and pore structure were detailedly characterized. To test the catalytic activity and selectivity of Ag@HKUST-1, eight kinds of olefins (1-hexene, cyclohexene, 1-octene, cyclooctene, styrene, 1-decene, 1, 1-diphenylethylene, and 1-dodecene) with different molecular sizes were hydrogenated in the presence of Ag@HKUST-1. To our delight, the olefins with molecular smaller than 5.0 Å exhibited excellent conversion, whereas those greater than 5.0 Å were rarely converted to the alkanes. After five recycles, the catalyst also displayed excellent catalytic activity in the hydrogenation of styrene, implying superior reusability of catalyst.

The morphology and microstructure of HKUST-1 and Ag@HKUST-1 crystals were investigated using SEM and TEM. The SEM and TEM images of the HKUST-1 (Figure 1a and b) show that octahedral crystals with diameter around 10 μm can be obtained. The overall morphology of the 0.1 mmol Ag@HKUST-1 (Figure 1c and d) is similar to that of the pristine crystals even loading Ag NPs by thermal reduction at 200 °C,

[1] W. J. Chen, B. H. Cheng, S. Q. Ting, Prof. H. Jiang
CAS Key Laboratory of Urban Pollutant Conversion, Department of
Chemistry, University of Science and Technology of China,
Hefei 230026, China
E-mail: jhong@ustc.edu.cn

suggesting little damage to the framework by the thermal treatment process. In addition, no obvious particles existed on the external surface of the 0.1 mmol Ag@HKUST-1, indicating that the Ag NPs were encapsulated by HKUST-1. Notably, the edge of the HKUST-1 shown in Figure 1d was smoothly and without impurities at the scale of 50 nm, implying the HKUST-1 crystals grow well.



As clearly seen from the TEM images and histograms of 0.05 mmol Ag@HKUST-1 and 0.1 mmol Ag@HKUST-1 (Figure 1e and f), there is no aggregation of Ag NPs, and large particles of Ag could hardly be seen in the wide range, indicating that Ag NPs are evenly dispersed. The average diameter of Ag NPs increases from 2.0 to 2.5 nm and the particle size distribution is also found to be narrow with the increase of the Ag dosages from 0.05 to 0.1 mmol. Noticeably, TEM images clearly show the Ag NPs are uniformly distributed in the network of HKUST-1 for Ag@HKUST-1 (Figure 1e and f). In addition, few Ag NPs exist on the edges of the HKUST-1, which confirms that Ag NPs have been embedded in the inner network of HKUST-1, and not been adsorbed on the external surface of HKUST-1. With the further increase of Ag dosage, the Ag NP size of 0.2 mmol Ag@HKUST-1 increased to diameter of 5.5 ± 1.2 nm (Figure 1g), and was larger than those of the above two due to the NPs tend to aggregation at high concentration. Most of the Ag NPs were limited in the interior of the HKUST-1 even though a small percentage of the NPs broke the framework and distributed on the edge of HKUST-1. However, for the 0.1 mmol Ag-HKUST-1 prepared by a traditionally impregnated process, most of the Ag NPs were adsorbed on the surface of HKUST-1, and some of Ag NPs randomly distributed on the surface and inner space of HKUST-1 after the thermal reduction. The particle size of Ag NPs is 19.2 ± 9.2 nm, showing that the aggregation of Ag NPs occurs during the thermal reduction process. Comparing Figure 1f and h with same Ag dosage and using double-solvents and impregnated method, respectively, the size and distribution of

Ag NPs are completely different, resulting in different size-selective catalytic effects for hydrogenation.

Figure 2 shows the N_2 adsorption-desorption isotherms and pore size distribution profiles of HKUST-1. The adsorption-desorption isotherm (Figure 2a) displayed a type I shape with high N_2 uptakes at relatively low pressures, indicating a characteristic microporous material. The specific surface area calculated by the Brunauer-Emmett-Teller (BET) method was $1145 \text{ m}^2/\text{g}$, and the total pore volume was $0.6476 \text{ cm}^3/\text{g}$. As shown in Figure 2b, pore size distribution curve of HKUST-1 analyzed by the nonlocal density functional theory (NLDFT) algorithm exhibited the maximum peaks at 0.5 and 0.9 nm. The 3D unit cell crystal framework of HKUST-1 is composed of square-shaped pores (diameter 9.0 Å) surrounded by small pockets (diameter 5.0 Å) (Figure S2). The pore size distribution of HKUST-1 is consistent with the reported literature.^[26] The slightly decreased surface area ($851 \text{ m}^2/\text{g}$) of 0.1 mmol Ag@HKUST-1 compared with parent HKUST-1 suggests that the cavities of the HKUST-1 frameworks are occupied by the highly dispersed Ag NPs (Figure S3). The pore size distribution of 0.1 mmol Ag@HKUST-1 is similar to HKUST-1, indicating the pore structure of HKUST-1 is maintained during the loading of Ag NPs.

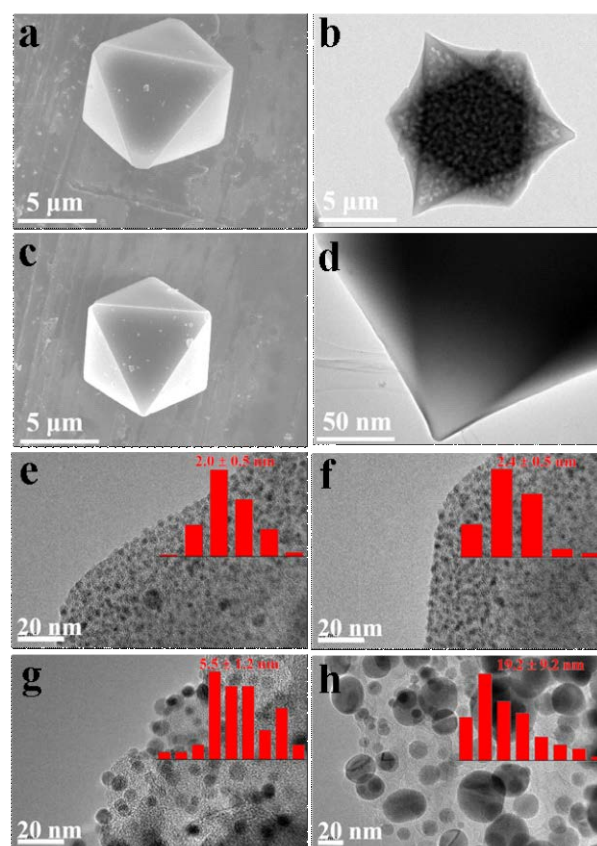


Figure 1 SEM images of (a) HKUST-1 and (c) 0.1 mmol Ag@HKUST-1; (b) and (d) TEM images of HKUST-1 with different scales; Representative TEM images of 0.05 mmol Ag@HKUST-1 (e), 0.1 mmol Ag@HKUST-1 (f), 0.2 mmol Ag@HKUST-1 (g); and 0.1 mmol Ag-HKUST-1 (h); inset (e-h) is the corresponding size distribution histograms of Ag NPs.

X-ray diffraction (XRD) was performed to verify the crystalline structure. Figure 2c shows the XRD pattern of HKUST-1 before and after thermal reduction. All the diffraction peaks of HKUST-1 in this study was essentially identical to that of previously reported results.^[27, 28] Further, the main diffraction peaks remained unchanged after thermal reduction at 200 °C under flowing H₂/Ar gas, clearly indicating that the crystal structure have not been destroyed, which is in agreement with the result of SEM. As shown in Figure 2d, the appearance of Ag diffraction peaks (JCPDS card no. 04-0783) suggests the formation of Ag NPs confined by HKUST-1. The characteristic peak of Ag at 2θ of 43.4° were observed in all Ag@HKUST-1, which can be attribute to (200) lattice plane of Ag with a face-centered cubic crystal structure.^[29] Another characteristic peak of Ag at 2θ of 38.3° (111) weakened and disappeared with the decrease of Ag dosages. For 0.1 mmol Ag-HKUST-1, the diffraction peak only appeared at 38.3°. indicating the only existence of (111) crystal face. Besides, all the diffraction peaks in the 2θ range of 5-30° are in good agreement with HKUST-1 (Figure 2d), which means the integrity of the HKUST-1 was maintained after Ag loading.

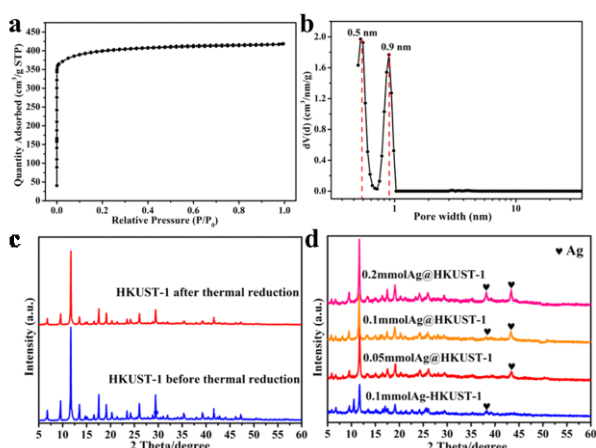


Figure 2 (a) N₂ adsorption-desorption isotherms and (b) pore diameter distribution profiles of HKUST-1. (c) XRD patterns of HKUST-1 before and after thermal reduction; (d) XRD patterns of Ag supported by HKUST-1 with different methods and concentration of Ag.

Figure 3 shows the chemical composition in Ag@HKUST-1 as determined by XPS. Two characteristic peaks (Figure 3a) are observed at 933.20 and 953.14 eV, corresponding to the Cu 2p_{3/2} and Cu 2p_{1/2} states of Cu²⁺, respectively.^[30] In addition, the “shake-up-satellites” located at 939.95, 943.83, and 962.46 eV, indicating the presence of divalent Cu (II) species.^[31] As shown in Figure 3b, the two peaks at 368.53 and 374.64 eV with a spin-orbit separation of 6.0 eV, correspond to the binding energies of Ag 3d_{5/2} and Ag 3d_{3/2}. These two characteristic peaks of Ag 3d_{5/2} and Ag 3d_{3/2} are attributed to the Ag⁰ species,^[32] which clearly indicates the presence of zero-valent metallic Ag NPs and is consistent with the XRD results. The energy spectrum of electron C 1s reveal two surface components (Figure 3c). The peak at 284.81 and 288.65 eV are assigned to the binding energy value of the hydrocarbon C-C and the carboxylate carbon -COO, respectively. The peak of O 1s (Figure 3d) could

be deconvoluted into two peaks with binding energies of 531.81 and 532.55 eV, one from -C=O/-OH and the other from C-O-Cu.^[33] In addition, the relative content of major elements and the XPS survey spectra are displayed in Table S1 and Figure S4, and the contents of Ag NPs on the surface of 0.1mmol Ag@HKUST-1 is very low.

The thermal stability of HKUST-1 and Ag@HKUST-1 were studied by thermogravimetric analysis (TGA) from room temperature to 700 °C with a heating rate of 10 °C/min, and the result was shown in Figure 4a, and the Derivative-Thermogravimetry (DTG) was displayed in Figure S5. The weight loss behavior of HKUST-1 and Ag@HKUST-1 can be divided into two major steps. The first weight loss stage occurs at temperatures below 130 °C, which are associated with the loss of free molecules physically absorbed in the micropores and the weight loss depends on the initial degree of solvation of the materials. Comparing with the HKUST-1, the weight loss ratio of the Ag@HKUST-1 was only 11.33% as most water and solvent molecules were removed from the surface and pores of HKUST-1 during the thermal reduction at 200 °C under flowing H₂/Ar gas. Notably, for HKUST-1 and Ag@HKUST-1, a platform stage can be observed after the removal of solvent, indicating the stability of the frameworks of the HKUST-1 crystals in this temperature range. The 0.01 mmol Ag@HKUST-1 has a slightly different onset decomposition temperature (125 °C) from HKUST-1 (130 °C). The second weight loss begins at 315 °C for HKUST-1 crystals and ends around 370 °C, while the onset decomposition temperature of the Ag@HKUST-1 is approximately 35 °C lower than that of the HKUST-1. This phenomenon may be caused by the decomposition of organic ligands expedited by the small-size and active Ag NPs.^[34] The organic frameworks are initially decomposed at 370 °C and completely carbonized at higher temperature under N₂ atmosphere. TGA analysis indicates that using low-temperature thermal reduction at 200 °C under flowing H₂/Ar gas can obtain Ag NPs while effectively maintains the structure of the HKUST-1.

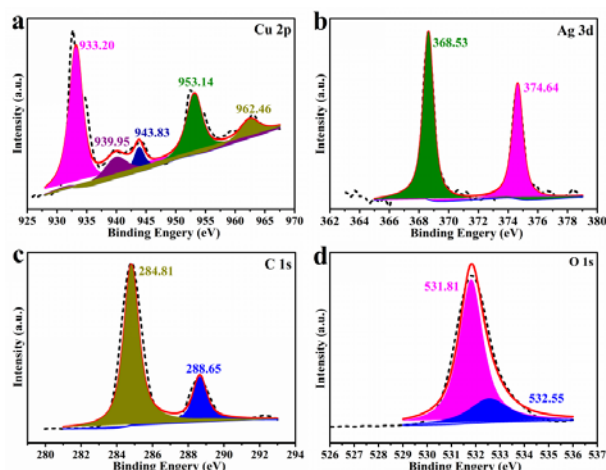


Figure 3 XPS spectra of the Ag@HKUST-1. (a) Cu 2p spectra; (b) Ag 3d spectra; (c) C 1s spectra; (d) O 1s spectra.

Hydrogen temperature-programmed reduction (H₂-TPR) was employed to study the reductive behavior of HKUST-1-

supported Ag ions. Combined with the TGA curves (Figure 4a), the upper critical temperature of TPR measurement was set to 280 °C to prevent the decomposition of the HKUST-1. From Figure 4b, no noticeable peak in pure HKUST-1 was detected, indicating the stability of the HKUST-1 under the reduced atmosphere (H_2 -Ar mixture gas) in the range of 30-280 °C. As displayed in Figure 4b, 0.1 mmol Ag^+ -HKUST-1 shows only one reduction peak at 210 °C which is attributed to the reduction of monovalence Ag species to metallic Ag.^[35] Similar to 0.1 mmol Ag^+ -HKUST-1, 0.05 mmol Ag^+ -HKUST-1, 0.1 mmol Ag^+ -HKUST-1, and 0.2 mmol Ag^+ -HKUST-1 also show a broad peak in the range of 130-230 °C located around a central peak of 205 °C corresponded to the $Ag^+ \rightarrow Ag^0$ reduction. Considering the results of the TGA and H_2 -TPR, the low-temperature thermal reduction of Ag ions to Ag NPs at 200 °C under flowing H_2/Ar is reasonable and effective. While Ag ions were reduced to Ag NPs, the structure of the HKUST-1 was retained, which is conducive to obtain small diameter of Ag NPs with high activity and large molecular sieving capability. These results can be confirmed by XRD, SEM, and TEM analyses.

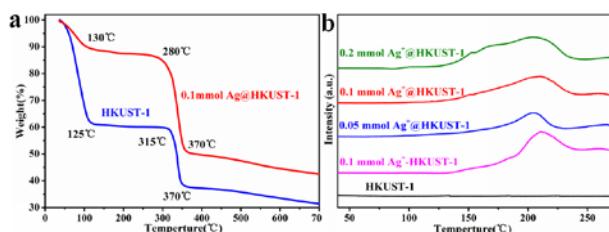


Figure 4 (a) TGA curves of HKUST-1 and 0.1 mmol Ag@HKUST-1; (b) H_2 -TPR of HKUST-1, 0.1 mmol Ag^+ -HKUST-1, 0.05 mmol Ag^+ -HKUST-1, 0.1 mmol Ag^+ -HKUST-1 and 0.2 mmol Ag^+ -HKUST-1.

HKUST-1 is a microporous material with uniform pores and unique porous channel, while the Ag NPs with small diameter exhibit excellent catalytic performance for hydrogenation. Combining the catalytic property of Ag NPs and the molecular sieving capability of HKUST-1, Ag@HKUST-1 may possess size-selective catalytic property. The size-selective catalytic property of HKUST-1 confined Ag NPs were tested in the hydrogenation of alkenes with different molecular diameters. As shown in Figure 5a, compared with eight different olefins, the hydrogenation efficiency displays a great diversity. All of Ag@HKUST-1 catalysts exhibit excellent catalytic performance to the hydrogenation of 1-hexene, 1-octene, cyclohexene and styrene, and the hydrogenation conversion rate increases with the increase of Ag content in the catalysts, suggesting the active site is a dominant factor for hydrogenation. However, an obvious difference was observed in the hydrogenation of 1-decene, cyclooctene, diphenylethylene and 1-dodecene by different Ag@HKUST-1 catalysts. 0.05 mmol Ag@HKUST-1 and 0.1 mmol Ag@HKUST-1 exhibit extremely low catalytic activity for hydrogenation of these olefins, which may be mainly attributed to the difference in the molecular size of the reaction substrate. The structure diagram and molecular size of olefins were listed in Table S2. It is strange that the 0.2 mmol Ag@HKUST-1 shows 13% conversion for 1-decene, 11% for cyclooctene, 4% for diphenylethylene, and 10% for 1-dodecene under the same catalytic condition and the content of reaction substrates. This

interesting phenomenon can be explained from Figure 1g. While most of the Ag NPs were limited in the interior of the HKUST-1, a small percentage of the Ag NPs located at the edge breaking the framework. The small amounts of Ag NPs appearing on the surface of HKUST-1 can provide low catalytic activity for large size olefins such as 1-decene, cyclooctene, diphenylethylene, and 1-dodecene.

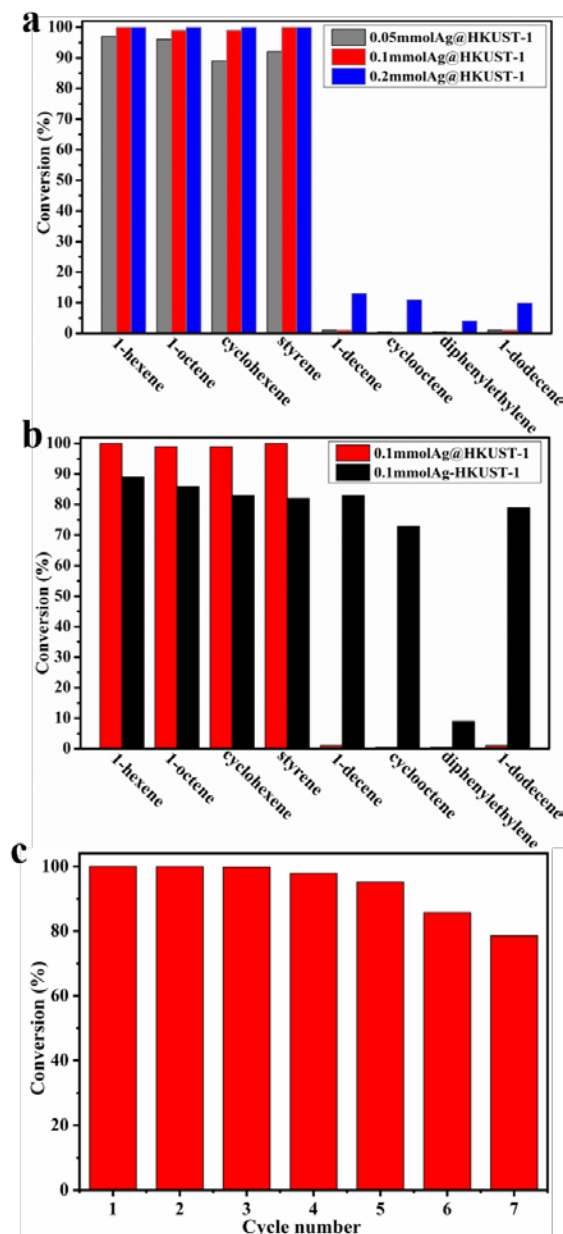


Figure 5 (a) Catalytic performance of Ag@HKUST-1 for the liquid-phase hydrogenation of different olefins; (b) Catalytic performance of Ag-HKUST-1 and Ag@HKUST-1 for the liquid-phase hydrogenation of different olefins; (c) Reusability of 0.1 mmol Ag@HKUST-1. Reaction conditions: 1 mmol styrene, 10 mL of CH_3OH , 1 MPa H_2 at 100 °C for 3 h with magnetic stirring. Color code: 0.05 mmol Ag@HKUST-1 (gray), 0.1 mmol Ag@HKUST-1 (red), 0.1 mmol Ag-HKUST-1 (black), 0.2 mmol Ag@HKUST-1 (blue).

In order to demonstrate the size-selective catalytic properties of the 0.1 mmol Ag@HKUST-1 synthesized by double-solvents method, the 0.1 mmol Ag-HKUST-1 prepared by an impregnated process was also tested in liquid-phase hydrogenation of olefins with different molecular sizes. Under the same reaction conditions, the 0.1 mmol Ag-HKUST-1 can catalytically convert 70-90% of seven olefins except diphenylethylene (9% conversion) to corresponding alkanes (Figure 5b). The extremely low conversion of diphenylethylene is mainly due to its conjugation effect which increases the difficulty of hydrogenation. It shows that Ag-HKUST-1 has no catalytic selectivity for the hydrogenation of olefins with different sizes. Furthermore, the conversion of 1-hexene, 1-octene, cyclohexene, and styrene by 0.1 mmol Ag-HKUST-1 is lower than that by 0.1 mmol Ag@HKUST-1. It is mainly ascribed to the much smaller size of Ag NPs in 0.1 mmol Ag@HKUST-1 (2.5 nm) compared to that in 0.1 mmol Ag-HKUST-1 (19.2 nm), which exhibit higher hydrogenation activity. The randomly distributed Ag NPs on the surface of 0.1 mmol Ag-HKUST-1 can provide hydrogenation activity sites for large-sized olefins (1-decene, cyclooctene, diphenylethylene, and 1-dodecene), and thus exhibit high conversion rate for these olefins. In contrast, the Ag NPs embedded in the inner network of HKUST-1 are not able to interact with large-size olefins, therefore the conversion rates of these olefins by 0.1 mmol Ag@HKUST-1 are very low. These results clearly demonstrate the molecular size-selective property of the 0.1 mmol Ag@HKUST-1. To further confirm the activity of Ag NPs on HKUST-1, the initial turnover frequency (TOF) value of the catalysts with different synthesis method is calculated (Table S3). The TOF of 0.1 mmol Ag@HKUST-1 (120 h^{-1}) is higher than that of 0.1 mmol Ag-HKUST-1, which may be attributed to the ultrafine Ag NPs confined in HKUST-1. Compared with other noble metal catalysts, the catalyst of 0.1 mmol Ag@HKUST-1 has outstanding catalytic efficiency relative to cost. To demonstrate the effect of confined pores of HKUST-1 on the selective hydrogenation of olefins, Ag NPs-C obtained by the same conditions as HKUST-1 was also used for the hydrogenation of olefins. It can be clearly seen from the Figure S6 that the hydrogenation conversion of HKUST-1 is low. The Ag NPs-C as hydrogenation catalyst exhibits good catalytic performance for olefins except diphenylethylene due to the active Ag NPs (Figure S6). However, compared with 0.1 mmol Ag@HKUST-1, the Ag NPs-C exhibits low catalytic selectivity for 1-decene, cyclooctene, diphenylethylene, and 1-dodecene. In addition, the catalytic activity of the Ag NPs-C is not as good as that of 0.1 mmol Ag@HKUST-1. This indicates that the confined pore of HKUST-1 played an important role in the selective hydrogenation of olefins.

Leaching of active components in the reaction liquid should be taken into consideration, which relates to the homogeneous and heterogeneous catalysis. The reaction mixture was hot filtered by centrifugation from the mixture after 1 h of reaction, the conversion of styrene did not increase during the subsequent reaction under the same catalytic conditions, indicating that no leaching of the catalyst occurred and the process is truly heterogeneous (Figure S7).

HKUST-1 has large pores of 9.0 Å which are accessible through small apertures of 5.0 Å.^[22] The uniform pore distributions could afford the ability of molecular size-selective catalysis. Eight kinds of olefins were divided into two groups according to whether the molecular size is greater than 5.0 Å. The molecular sizes of 1-hexene, 1-octene, cyclohexene, and styrene are smaller than 5.0 Å, and the group of olefins are small enough to diffuse through the pore apertures of HKUST-1 (5.0 Å) without serious hindrance; however, another group of olefins (1-decene, cyclooctene, diphenylethylene, and 1-dodecene) are much bigger than the pore apertures. Therefore, the hydrogenation conversion of two groups was significantly different by the 0.1 mmol Ag@HKUST-1. The Ag NPs synthesized by double-solvents method possess small and uniform size, which endow them high catalytic activity for hydrogenation of olefins. Meanwhile, these Ag NPs are confined in the interior of the HKUST-1, which could improve the stability and reusability of the catalyst.

The recycling test using styrene as model reactant was conducted to demonstrate the stability of 0.1 mmol Ag@HKUST-1 without any post treatment (Figure 5c). In the initial three cycles, sufficient catalytic activity could be preserved and styrene can be nearly completely converted (>99%). After five recycles, the catalytic performance slightly decreased until to seventh run, indicating that 0.1 mmol Ag@HKUST-1 has good reusability. Loss of the active component is a main cause of catalyst deactivation in liquid phase reactions. The high catalytic performance of 0.1 mmol Ag@HKUST-1 was maintained after two times of reuse, but decreased after six times of reuse. During the recycling, the intensity of peaks of metallic Ag decreased (Figure S8a), suggesting the leaching of the active metal. After six times of reuse (seven cycles), the Ag content in catalyst dropped from 3.2 wt% to 1.8 wt% (Figure S8b), coinciding with the XRD analysis.

In summary, we successfully prepared the ultrafine Ag NPs confined by HKUST-1 using double-solvent approach and the as-prepared catalyst exhibited much higher catalytic activity and selectivity for hydrogenation of olefins than Ag-HKUST-1 prepared by impregnated process. The olefins with molecular smaller than 5.0 Å were efficiently converted to the corresponding alkanes by Ag@HKUST-1, whereas those greater than 5.0 Å exhibited extremely low conversion. The catalytic performance of Ag@HKUST-1 slightly decreased using styrene as model reactant after five recycles, indicating that catalyst has good reusability.

Experimental section

The materials and methods are described in Supporting Information.

Acknowledgements

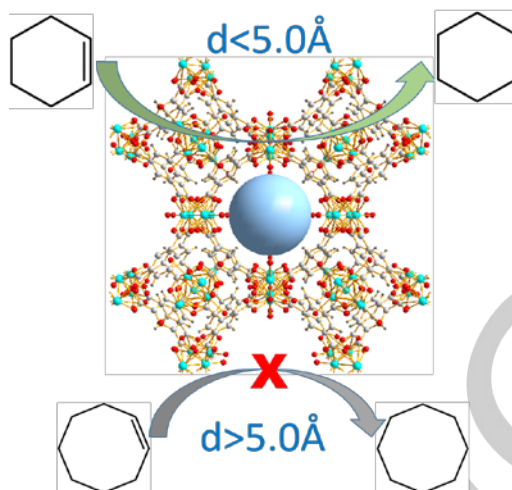
The authors gratefully acknowledge financial support from National Natural Science Foundation of China (21677138), Program for

Changjiang Scholars and Innovative Research Team in University "PCSIRT, the Key Special Program on the S&T for the Pollution Control, and Treatment of Water Bodies (No.2012ZX07103-001).

Keywords: HKUST-1 • Ag NPs • double-solvents method • size-selective • hydrogenation

- [1] S. G. Modha, M. F. Greaney, *J. Am. Chem. Soc.* **2015**, *137*, 1416-1419.
- [2] S. Prakash, K. Muralirajan, C. H. Cheng, *Angew. Chem. Int. Edit.* **2016**, *55*, 1844-1848.
- [3] M. Dhiman, V. Polshettiwar, *J. Mater. Chem. A* **2016**, *4*, 12416-12424.
- [4] H. Sun, Z. G. Liu, S. Chen, X. Quan, *Chem. Eng. J.* **2015**, *15*, 889-896.
- [5] S. Aguado, S. E. Jamal, F. Meunier, J. Canivet, D. Farrusseng, *Chem. Commun.* **2016**, *52*, 7161-7163.
- [6] W. N. Zhang, G. Lu, C. L. Cui, Y. Y. Liu, S. Z. Li, W. J. Yan, C. Xing, Y. R. Chi, Y. H. Yang, F. Huo, *Adv. Mater.* **2014**, *25*, 4056-4060.
- [7] L. N. Chen, H. Q. Li, M. W. Yan, C. F. Yuan, W. W. Zhan, Y. Q. Jiang, Z. X. Xie, Q. Kuang, L. S. Zheng, *Small* **2017**, *13*, 1700683.
- [8] T. M. Lima, C. G. S. Lima, A. K. Rathi, M. B. Gawande, J. Tucek, E. A. U. González, R. Zbořil, M. W. Paixão, R. S. Varma, *Green Chem.* **2016**, *18*, 5586-5593.
- [9] F. Wang, C. Liu, G. Liu, W. X. Li, J. H. Liu, *Catal. Commun.* **2015**, *2*, 142-146.
- [10] J. Zhang, L. Wang, Y. Shao, Y. Wang, B. C. Gates, F. S. Xiao, *Angew. Chem. Int. Ed.* **2017**, *56*, 9747-9751.
- [11] Q. L. Zhu, Q. Xu, *Chem. Soc. Rev.* **2014**, *43*, 5468-5512.
- [12] C. B. He, D. M. Liu, W. B. Lin, *Chem. Rev.* **2015**, *115*, 11079-11108.
- [13] G. W. Xu, Y. P. Wu, W. W. Dong, J. Zhao, X. Q. Wu, D. S. Li, Q. C. Zhang, *Small* **2017**, *13*, 1602996.
- [14] J. W. Zhang, C. C. Zhao, Y. P. Zhao, H. Q. Xu, Z. Y. Du and H. L. Jiang, *CrystEngComm* **2014**, *16*, 6635-6644.
- [15] J. Liang, Z. Liang, R. Zou, Y. L. Zhao, *Adv. Mater.* **2017**, *29*, 1701139.
- [16] Y. P. Wu, G. W. Xu, W. W. Dong, J. Zhao, D. S. Li, J. Zhang, X. H. Bu, *Inorg. Chem.* **2017**, *56*, 1402-1411.
- [17] G. Lu, S. Z. Li, Z. Guo, O. K. Farha, B. G. Hauser, X. Y. Qi, Y. Wang, X. Wang, S. Y. Han, X. G. Liu, J. S. DuChene, H. Zhang, Q. C. Zhang, X. D. Chen, J. Ma, S. C. J. Loo, W. D. Wei, Y. H. Yang, J. T. Hupp, F. W. Huo, *Nat. Chem.* **2012**, *4*, 310-316.
- [18] M. T. Zhao, K. Yuan, Y. Wang, G. D. Li, J. Guo, L. Gu, W. P. Hu, H. J. Zhao, Z. Y. Tang, *Nature* **2016**, *539*, 76-80.
- [19] L. Y. Chen, R. Luque, Y. W. Li, *Chem. Soc. Rev.* **2017**, *46*, 4614-4630.
- [20] Q. H. Yang, Q. Xu, S. H. Yu, H. L. Jiang, *Angew. Chem. Int. Ed.* **2016**, *55*, 3685-3689.
- [21] S. Hermes, M. K. Schröter, R. Schmid, L. Khodeir, M. Muhler, A. Tissler, R. W. Fischer, R. A. Fischer, *Angew. Chem. Int. Ed.* **2005**, *44*, 6237-6241.
- [22] Q. H. Yang, Q. Xu, H. L. Jiang, *Chem. Soc. Rev.* **2017**, *46*, 4774-4808.
- [23] X. H. Liu, J. G. Ma, Z. Niu, G. M. Yang, P. Cheng, *Angew. Chem. Int. Ed.* **2015**, *54*, 988-991.
- [24] Y. Z. Chen, Q. Xu, S. H. Yu, H. L. Jiang, *Small* **2015**, *11*, 71-76.
- [25] A. Aijaz, A. Karkamkar, Y. J. Choi, N. Tsumori, E. Ronnebro, T. Autrey, H. Shioyama, Q. Xu, *J. Am. Chem. Soc.* **2012**, *134*, 13926-13929.
- [26] Y. Yang, P. Shukla, S. B. Wang, V. Rudolph, X. M. Chen, Z. H. Zhu, *RSC Adv.* **2013**, *3*, 17065-17072.
- [27] L. He, L. F. Dumeé, D. Liu, L. Velleman, F. H. She, C. Banos, J. B. Davies, L. X. Kong, *RSC Adv.* **2015**, *5*, 10707-10715.
- [28] M. Mazaj, T. Čendak, G. Buscarino, M. Todaro, N. Z. Logar, *J. Mater. Chem. A* **2017**, *5*, 22305-22315.
- [29] K. Tian, W. J. Liu, H. Jiang, *ACS Sustainable Chem. Eng.* **2015**, *3*, 269-276.
- [30] Y. T. Wang, Y. Y. Lu, W. W. Zhan, Z. X. Xie, Q. Kuang, L. S. Zheng, *J. Mater. Chem. A* **2015**, *3*, 12796-12803.
- [31] E. G. Garrido-Ramírez, J. F. Marco, N. Escalona, M. S. Ureta-Zañartu, *Micropor. Mesopor. Mat.* **2016**, *22*, 303-311.
- [32] W. J. Liu, L. L. Ling, Y. Y. Wang, H. He, Y. R. He, H. Q. Yu, H. Jiang, *Environ. Sci.: Nano* **2016**, *3*, 745-753.
- [32] G. W. Zhan, H. C. Zeng, *Adv. Funct. Mater.* **2016**, *26*, 3268-3281.
- [34] S. X. Gao, N. Zhao, M. H. Shu, S. N. Che, *Appl. Catal. A.* **2010**, *388*, 196-201.
- [35] X. L. Deng, M. X. Li, J. Zhang, X. Y. Hu, J. B. Zheng, N. W. Zhang, B. H. Chen, *Chem. Eng. J.* **2017**, *1*, 544-555.

The synthesis of Ag NPs confined by MOF (Ag@HKUST-1) using double-solvent approach using HKUST-1, and applied it for size-selective hydrogenation of olefins.



Wen-Jing Chen, Xiao-Qing Liu, Shun Zhang, and Hong Jiang*

Page No. – Page No.

Preparation of MOF confined Ag NPs with narrow cage size distribution for high size selective hydrogenation of olefins

Accepted Manuscript